Electronic Supplementary Material (ESI) for Catalysis Science & Technology.

SUPPLEMENTARY INFORMATION

Cobalt-containing zeolitic imidazole frameworks for C-H activation using visible-light redox photocatalysis

M. E. Potter[a*ϕ], C. P. Ross[a,bϕ], D. Gianolio[c], R. Rios[a] and R. Raja[a*]

a) Chemistry Department, University of Southampton, Southampton, SO17 1BJ, UK.

b) Institute of Chemical and Engineering Sciences (ICES), Agency for Science, Technology and Research (A*STAR), Neuros, 8 Biomedical Grove, Singapore 138665.

c) Diamond Light Source, Harwell, Oxfordshire, OX11 0FA, UK.

ϕ These authors contributed equally.

*M.E.Potter@soton.ac.uk

Contents

Confirming the structural integrity Page S2

Exploring the local coordination environment Page S4

Reactant synthesis Page S9

References Page S11

Confirming the structural integrity

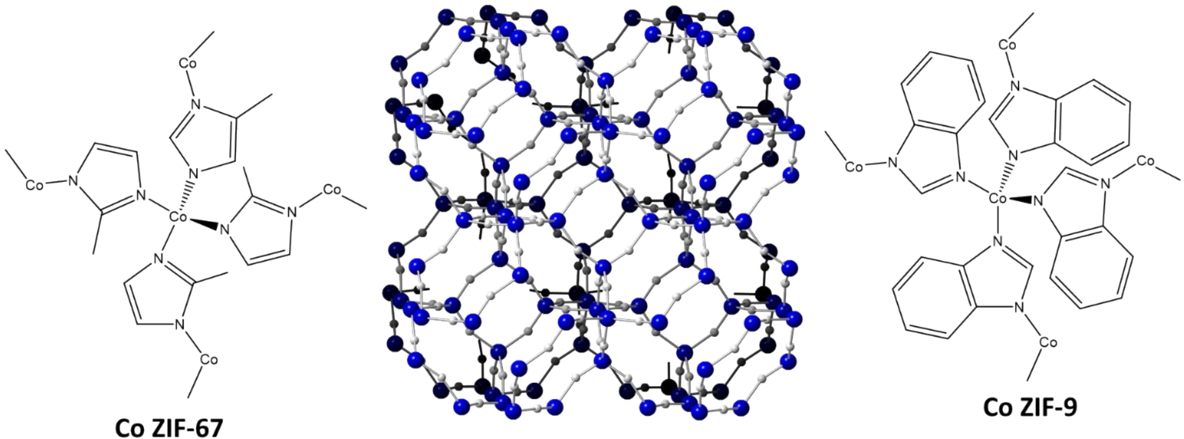

Co ZIF-67

Sodalite (SOD) framework

Co ZIF-9

Fig. S1 Showing the differences between ZIF-9 and ZIF-67 architecture with the sodalite (SOD) framework. Here the blue atoms represent cobalt, and the white balls represent the organic linker, for ZIF-67 this is 2-methylimidazole, for ZIF-9 it is benzylimidazole.

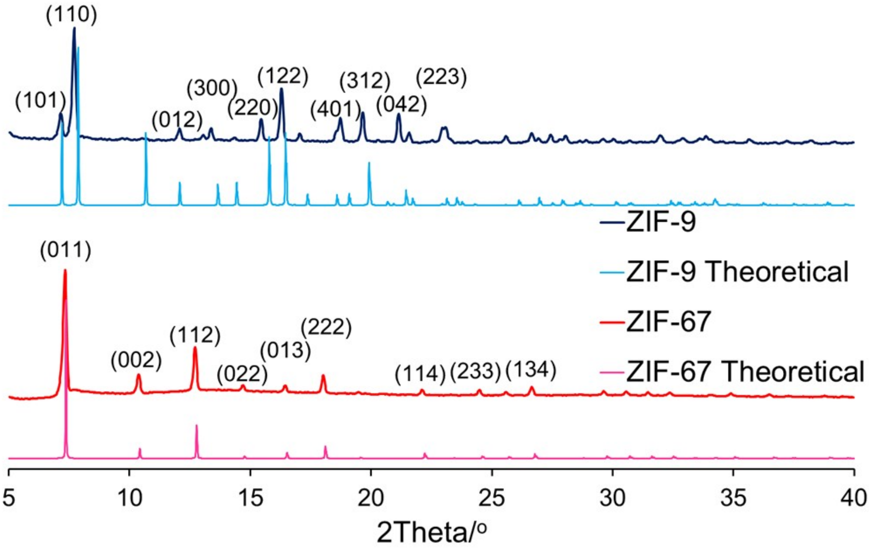

Fig. S2 Powder XRD of the cobalt-ZIF samples showing phase purity and crystallinity, compared to theoretical XRD patterns generated from cif files for Co ZIF-9[S1,S2] and Co ZIF-67[S3,S4].

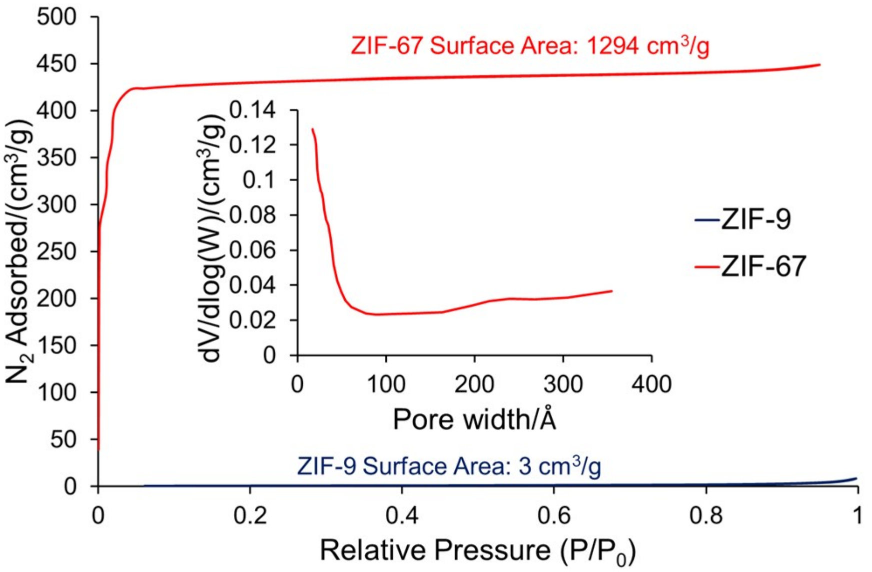

Fig. S3 N$_2$ physisorption plot of the cobalt-ZIF samples at 77 K, with BJH pore distribution plot of ZIF-67 (inset) confirming the purely microporous network.

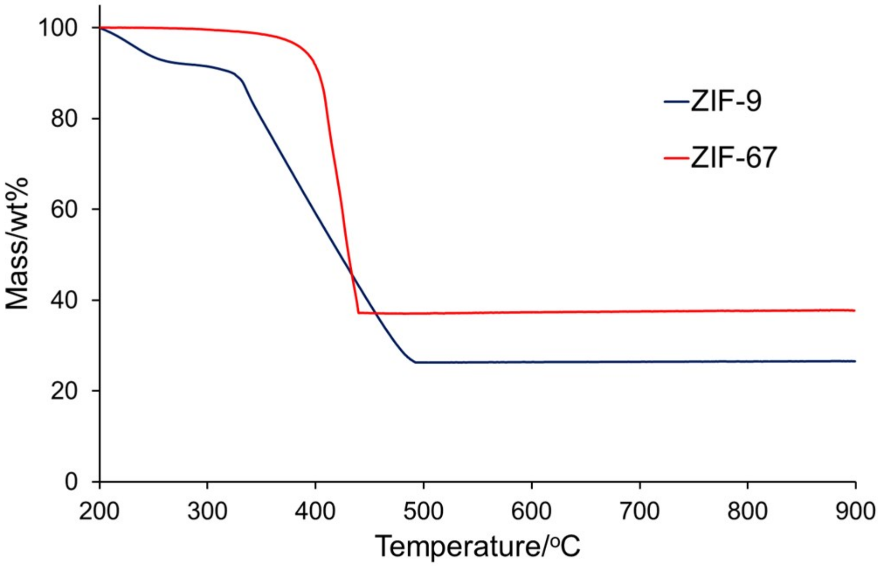

Fig. S4 Thermogravimetric curve of the three cobalt-ZIF samples. 50 ml/min air, 10 °C/minute ramp rate, 10 ml/min He carrier.

Table S1 ICP loading of Cobalt containing ZIFs.

	Theoretical Mass / wt%	ICP Analysis / wt%
ZIF-9	20.1 (18.2 with DMF)	18.6
ZIF-67	26.7	26.2

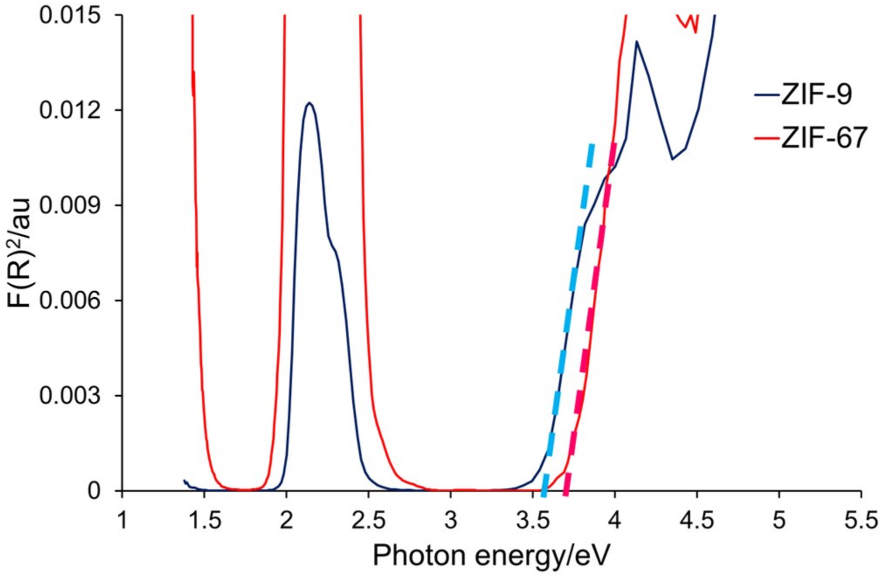

Fig. S5 Estimating the band gap of Co ZIF-9 and Co ZIF-67, using the Kubelka-Munk function as 3.6 eV (ZIF-9) and 3.7 eV (ZIF-67).

Exploring the local coordination environment

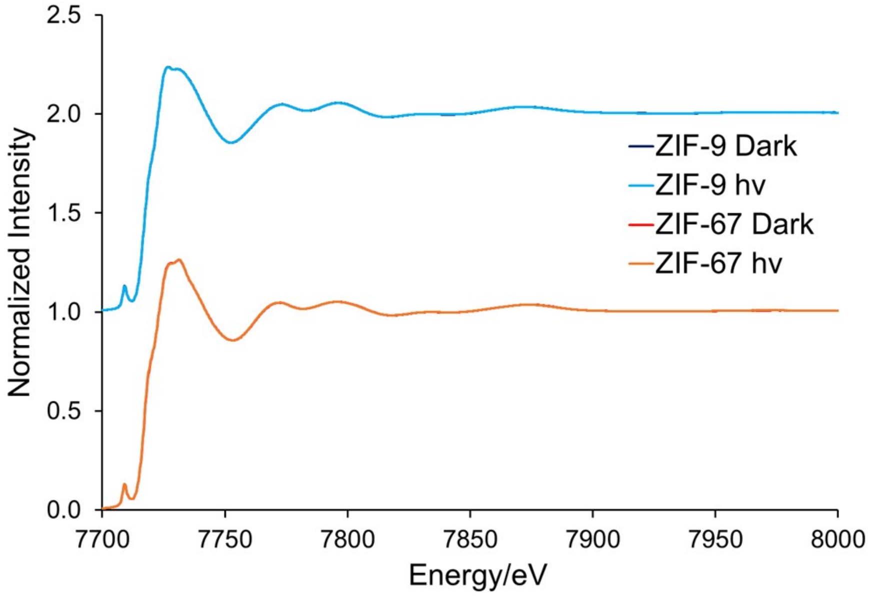

Fig. S6 Normalized EXAFS spectra for ZIF-9 and ZIF-67 Nano, showing the similarity under 'Dark' and 'hv' conditions, both ZIF-9 spectra have been increased by a normalized intensity of 1.0 for ease of comparison. Note, the similarities between 'hv' and 'Dark' spectra mean they are essentially super-imposed on this scale.

Table S2 IFEFFIT modelling results for ZIF-9 and ZIF-67.

ZIF-9 Dark

Abs Sc	N	R/Å	$2\sigma^2$/Å^2	E_f/eV	R_{Factor}
Co-N	4	2.00(1)	0.005(1)	4.18(77)	0.023
Co-C1	4	2.98(3)	0.009(8)		
Co-C2	3	3.04(14)	0.036(46)		

ZIF-9 hv

Abs Sc	N	R/Å	$2\sigma^2$/Å^2	E_f/eV	R_{Factor}
Co-N	4	2.00(1)	0.005(1)	4.16(73)	0.024
Co-C1	4	2.99(3)	0.010(8)		
Co-C2	3	3.03(17)	0.040(53)		

ZIF-67 Dark

Abs Sc	N	R/Å	$2\sigma^2$/Å^2	E_f/eV	R_{Factor}
Co-N	4	2.00(1)	0.005(1)	4.50(89)	0.030
Co-C	8	3.00(2)	0.013(4)		
Co-C-N	16	3.12(10)	0.070(42)		

ZIF-67 hv

Abs Sc	N	R/Å	$2\sigma^2$/Å^2	E_f/eV	R_{Factor}
Co-N	4	2.00(1)	0.006(1)	4.36(86)	0.028
Co-C	8	3.00(2)	0.015(5)		
Co-C-N	16	3.12(10)	0.075(44)		

Fitting parameters: $S_0^2 = 0.77$, as deduced by Co(0) foil. Fit range: $2.6 < k < 12.0$, $1.0 < R < 2.8$, number of independent points: 10.6. Fitted in k^1, k^2 and k^3 spaces simultaneously.

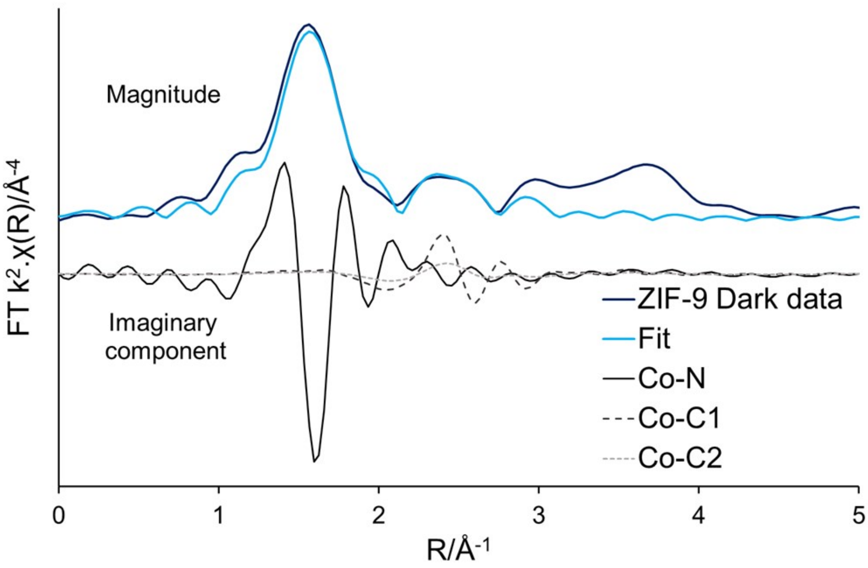

Fig. S7 Magnitude and imaginary component of the k^2 weighted Fourier transform EXAFS data for ZIF-9 under 'dark' conditions, showing the influence of different fitted paths.

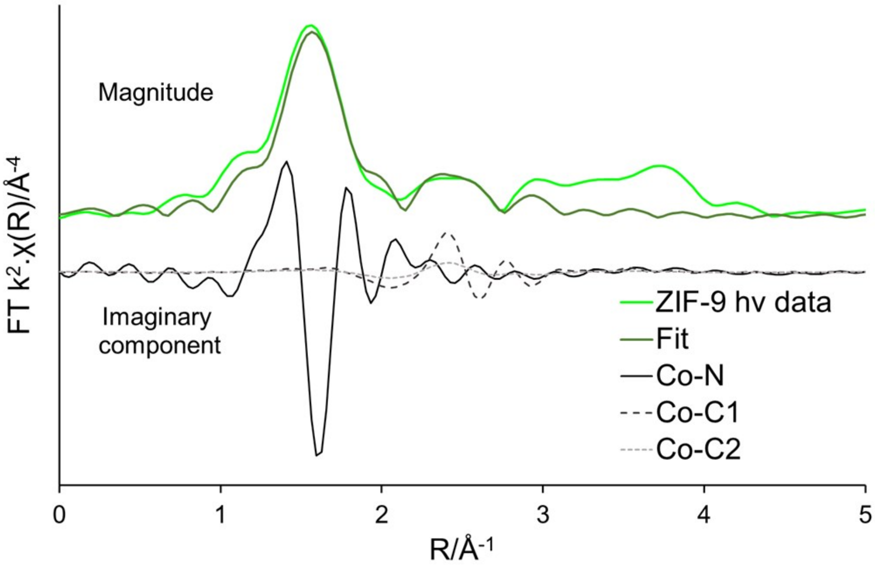

Fig. S8 Magnitude and imaginary component of the k^2 weighted Fourier transform EXAFS data for ZIF-9 under 'hv' conditions, showing the influence of different fitted paths.

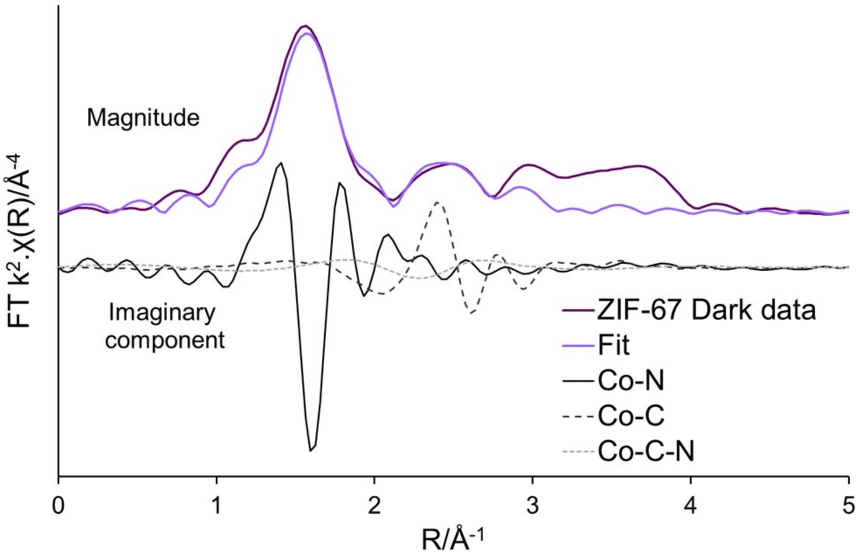

Fig. S9 Magnitude and imaginary component of the k^2 weighted Fourier transform EXAFS data for ZIF-67 under 'dark' conditions, showing the influence of different fitted paths.

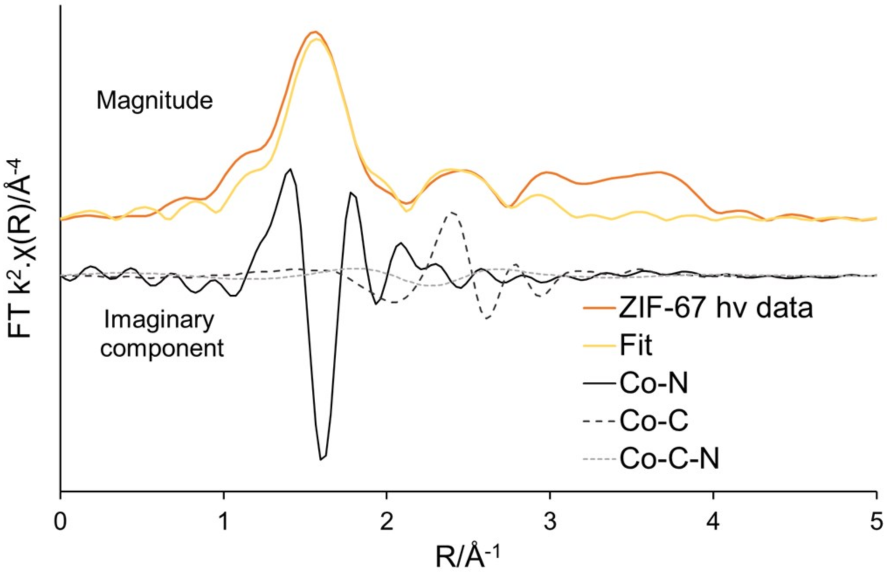

Fig. S10 Magnitude and imaginary component of the k^2 weighted Fourier transform EXAFS data for ZIF-67 under ‘hv’ conditions, showing the influence of different fitted paths.

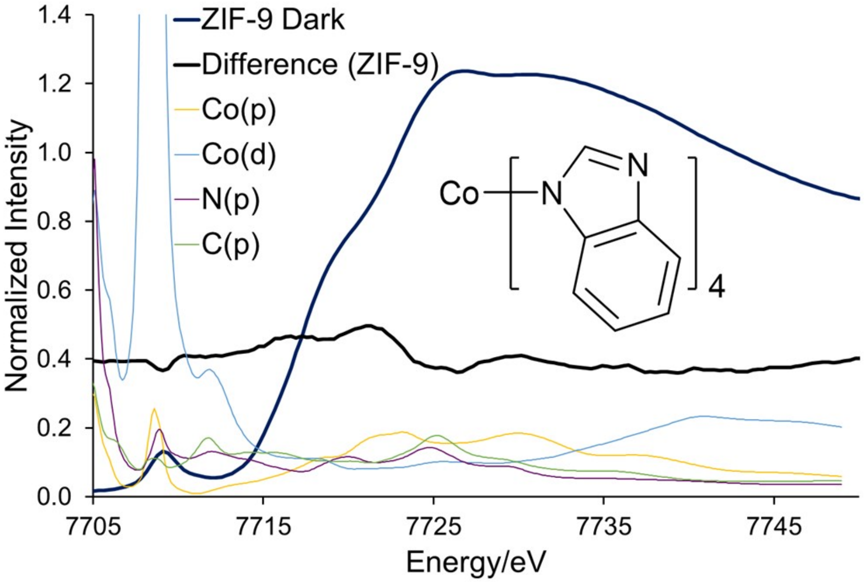

Fig. S11 Density of states simulation results for ZIF-9, from the crystallographic structure of ZIF-9, showing the contributions from each orbital set. The difference spectrum is scaled by a factor of 20 and incremented by 0.4 for ease of observation.

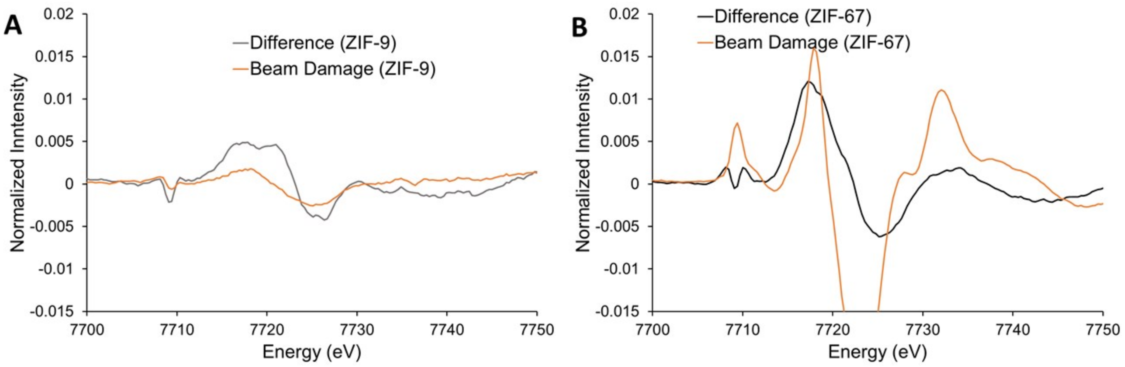

Fig. S12 Contrasting the beam damage (Dark Rerun – Dark Final) with the difference (Light – Dark Initial). Here we see the ZIF-9 is barely affected by beam damage, confirming the changes on exposure to light are genuine. If ZIF-67 we see different changes for beam damage to light exposure again confirming the changes to light are genuine.

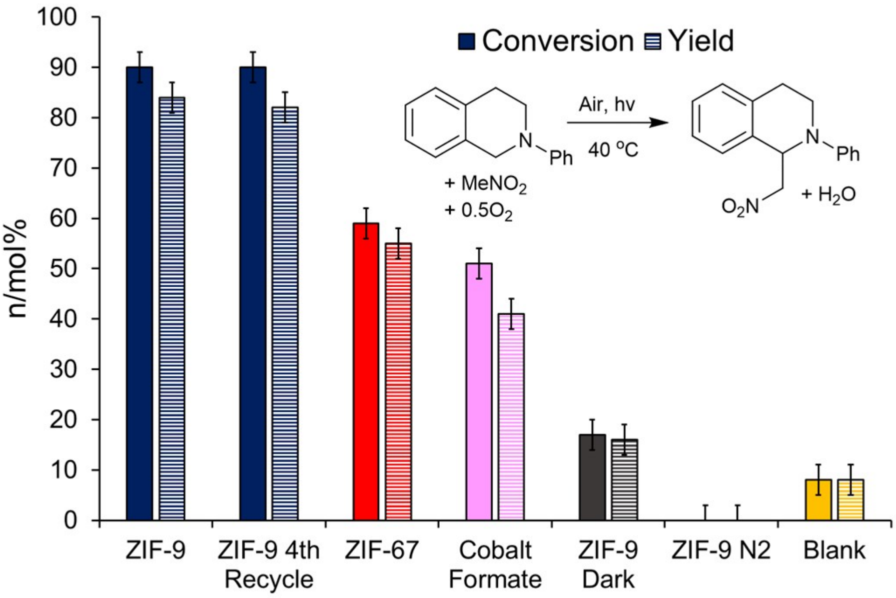

Fig. S13 Photocatalytic activity of cobalt-containing ZIFs and control reactions. Reaction conditions: PhTHIQ (0.11 mmol) and catalyst (10 wt%) were stirred in nitromethane (1 mL), with mesitylene as an internal 1H NMR standard, for 6 h at 40 °C, using a solar simulator with a 515 nm High-Pass band filter. 'Conversion' = Conversion of reactant. 'Yield' = Yield of product. Errors are estimated as ± 3 mol% based on repeated measurements.

Reactant synthesis

Synthesis of N-phenyl-1,2,3,4-tetrahydroisoquinoline (PhTHIQ), 1a

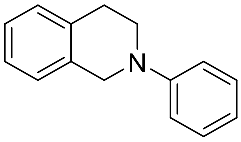

The procedure for the starting material used throughout the project was as follows:[S5] Copper (I) iodide, (476 mg, 2.50 mmol) and potassium phosphate (10.119 g, 47.7 mmol) were placed under an inert atmosphere before adding 2-propanol (23.8 mL), ethylene glycol (2.6 mL, 47.6 mmol), 1,2,3,4-tetrahydroisoquinoline (4.8 mL, 35.7 mmol) and iodobenzene (2.7 mL, 23.8 mmol). The reaction mixture was then heated to 90 °C and left stirring for 24 hours. Afterwards, it was left to cool to room temperature before adding diethyl ether (50 mL) and water (50 mL). The organic layer was extracted by diethyl ether (2 x 50 mL) before washing the combined organic phases with brine (50 mL) and drying over magnesium sulfate. The solvent was removed by rotary evaporation, the dark brown oil was purified by column chromatography on silica gel (hexane/ethyl acetate 19:1). The yield was recorded at 3.238 g, 65 %. A peach solid with R_f of 0.25 in the eluent mentioned.

^{1}H NMR (400 MHz, $CDCl_3$): δ 7.32-7.27 (2H, m), 7.21-7.14 (4H, m), 6.99 (2H, d, J = 8.0 Hz), 6.83 (1H, t, J = 7.3 Hz), 4.42 (2H, s), 3.57 (2H, t, J = 5.9 Hz), 3.00 (2H, t, J = 5.8 Hz)

^{13}C NMR (400 MHz, $CDCl_3$): δ 150.71, 135.03, 134.63, 129.34, 128.66, 126.67, 126.47, 126.16, 118.80, 115.29, 50.89, 46.67, 29.27

IR (thin film): 3055 cm^{-1} (s, sp^2 C-H), 2827 cm^{-1} (s, sp^3 C-H), 1598 cm^{-1} (m, benzene C=C), 1501 cm^{-1} (m, benzene C=C)

ESI-MS: *m/z* 210

In agreement with the published literature.[S5]

Synthesis of 2-(p-tolyl)-1,2,3,4-tetrahydroisoquinoline, 1b

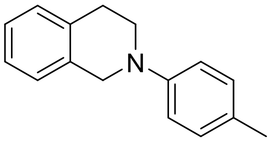

Synthesis procedure as per 1a, except a column eluent of hexane/ethyl acetate of 15:1 was used. The yield was 59 mol% of brown oil.

^{1}H NMR (400 MHz, $CDCl_3$): δ 7.62-7.39 (6H, m), 7.27 (2H, d, J = 8.5 Hz), 4.68 (2H, s), 3.81 (2H, t, J = 5.8 Hz), 3.29 (2H, t, J = 5.8 Hz), 2.67 (3H, s). In agreement with published literature.[S5]

Synthesis of 2-(4-methoxyphenyl)-1,2,3,4-tetrahydroisoquinoline, 1c

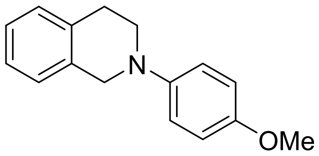

Synthesis procedure as per 1a, except a column eluent of hexane/ethyl acetate of 18:1 was used. The yield was 61 mol% of white powder.

^{1}H NMR (400 MHz, CDCl$_3$): δ 7.17 (4H, m), 7.00 (2H, d, J = 9.1 Hz), 6.89 (2H, d, J = 9.1 Hz), 4.32 (2H, s), 3.80 (3H, s), 3.46 (2H, t, J = 5.9 Hz), 3.00 (2H, t, J = 5.9 Hz). In agreement with published literature.[S5]

Synthesis of 2-(4-chlorophenyl)-1,2,3,4-tetrahydroisoquinoline, 1d

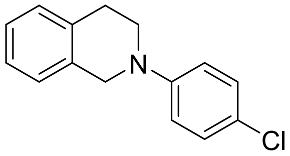

Synthesis procedure as per 1a, except a column eluent of hexane/ethyl acetate of 18:1 was used. The yield was 51 mol% of white powder.

^{1}H NMR (400 MHz, CDCl$_3$): δ 7.26-7.13 (6H, m), 6.92-6.86 (2H, m), 4.39 (2H, s), 3.54 (2H, t, J = 5.9 Hz), 2.99 (2H, t, J = 5.8 Hz). In agreement with published literature.[S5]

Synthesis of 2-(4-(trifluoromethyl)phenyl)-1,2,3,4-tetrahydroisoquinoline, 1e

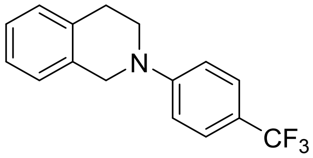

Synthesis procedure as per 1a, except a column eluent of hexane/ethyl acetate of 20:1 was used. The yield was 29 mol% of white powder.

^{1}H NMR (400 MHz, CDCl$_3$): δ 7.51 (2H, d, J = 8.6 Hz), 7.26-7.14 (4H, m), 6.95 (2H, d, J = 8.8 Hz), 4.50 (2H, s), 3.64 (2H, t, J = 5.9 Hz), 3.01 (2H, t, J = 5.8 Hz). In agreement with published literature.[S5]

Synthesis of 2-(2-fluorophenyl)-1,2,3,4-tetrahydroiqoquinoline, 1f

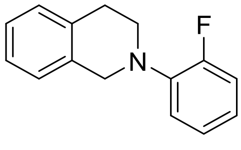

Synthesis procedure as per 1a, except a column eluent of hexane/ethyl acetate of 18:1 was used. The yield was 54 mol% of pale white crystalline powder.

^{1}H NMR (400 MHz, CDCl$_3$): δ 7.23-7.02 (7H, m), 6.99-6.92 (1H, m), 4.33 (2H, s), 3.47 (2H, t, J = 5.9 Hz), 3.01 (2H, t, J = 5.9 Hz). In agreement with published literature.[S5]

References

[S1] K. S. Park, Z. Ni, A. P. Côté, J. Y. Choi, R. Huang, F. J. Uribe-Romo, H. K. Chae, M. O’Keefe and O. M. Yaghi, CCDC 602543: Experimental Crystal Structure Determination, 2014, DOI: 10.5517/ccn6zwp.

[S2] K. S. Park, Z. Ni, A. P. Côté, J. Y. Choi, R. Huang, F. J. Uribe-Romo, H. K. Chae, M. O’Keefe and O. M. Yaghi, *Proc. Natl. Acad. Sci.*, 2006, **103**, 10186-10191.

[S3] R. Banerjee, A. Phan, B. Wang, C. Knobler, H. Furukawa, M. O’Keefe and O. M. Yaghi, CCDC 671074: Experimental Crystal Structure Determination, 2014, DOI: 10.5517/ccqj9k2.

[S4] R. Banerjee, A. Phan, B. Wang, C. Knobler, H. Furukawa, M. O’Keefe and O. M. Yaghi, *Science*, 2008, **319**, 939-943.

[S5] B. L. Korbad and S. H. Lee, *Chem. Commun.*, 2014, **50**, 8985-8988.